

# Modular Design of Long Narrow Scintillating Cells for ILC Detector

D. Beznosko<sup>1a</sup>, G. Blazey<sup>1</sup>, A. Dyshkant<sup>1</sup>, J. Maloney<sup>1</sup>, V. Rykalin<sup>1</sup>, J. Schellpfer<sup>2</sup>

<sup>1</sup>Northern Illinois University, Dekalb, IL 60115 USA

<sup>2</sup>Fermi National Acceleration Laboratories, Batavia, IL 60501 USA

## Abstract

The experimental results for the narrow scintillating elements with effective area about 20 cm<sup>2</sup> are reported. The elements were formed from the single piece of scintillator and were read out via wavelength shifting fibers with the MRS (Metal/Resistor/Semiconductor) photodiodes on both ends of each fiber. The formation of the cells from the piece of scintillator by using grooves is discussed. The cell performance was tested using the radioactive source by measuring the PMT current and a single rate after amplifier and discrimination with threshold at about three photo electrons in each channel and quad coincidences (double coincidences between sensors on each fiber and double coincidences between two neighboring fibers). This result is of high importance for large multi-channel systems, i.e. module may be used as an active element for calorimeter or muon system for the design of the future electron-positron linear collider detector because cell effective area can be smoothly enlarged or reduced (to 4 cm<sup>2</sup> definitely).

PACS-1996 codes: 29.40.Wk, 29.40.Mc, 29.40.Vj

Keywords: MRS photodiode, calorimeter, strip, extruded scintillator, coincidence trigger, multi-channel

---

<sup>a</sup> Corresponding Author: Dmitry Beznosko, 4107 47ave #3D, Sunnyside, NY, USA (telephone: 347-992-6486, email: dima@hitech.us).

## I. INTRODUCTION

The challenging goal of the future international electron-positron linear collider detector is to get about  $30\%/ \sqrt{E}$  jet energy resolution, or better. Nowadays, an energy flow algorithm is the most promising way; however, it demands highly granulated sampling hadron calorimeter. Because of large cost, a digital approach is under investigation for use in hadron calorimetry. The electronics for a digital hadron calorimeter should be less expensive than for an analog one. The active medium can be gas [1, 2] or solid, for example, small scintillation cells [3] or scintillator strip [4]. For millions of cells, the small area of the active element creates assembly issues, dead zones and edge effects that significantly reduce the efficiency of registration (smaller the area, longer the perimeter and, consequently, larger the edge effects).

We have tested a long narrow scintillating element with effective area about  $20 \text{ cm}^2$  using optical readout via wavelength (WLS) shifting fibers and miniaturized photo detectors. A set of those elements can be combined with another layer perpendicular to its orientation, thereby creating the space resolution of about  $1 \text{ cm}^2$  or better. Such elements, flexible in length and width, combine naturally in a set of 10 or more, drastically reducing the amount of dead zones and edge effects, and providing space for the small-sized photodetectors that are insensitive to strong magnetic field, like MRS (Metal/Resistor/Semiconductor) photodiode [5, 6], and on-board electronics assembly similar to [7], which may include amplifiers, discriminators, logic units, etc. In this way, usage of clear fiber can be avoided completely, WLS fibers are used in the minimum amount, and fiber routing problems are avoided. In the future, scintillating elements can be produced by extrusion process [8]. This note reports on the first promising indication for the similar cells performs with machining grooves that were tested using  $^{90}\text{Sr}$  radioactive source by measuring current and rate.

## II. GENERAL DESIGN CONSIDERATIONS

The main idea behind the work done is to create a module-based self-triggering and self-sufficient detector part with an area resolution of about  $1 \text{ cm}^2$  or less, flexible in length and width, that already consists of several cells, fibers, photodetectors and necessary on-board electronics. The ideas tested in this paper are: creation of the cell-like elements and their possible optical separation within solid scintillator piece using grooves, use of miniature solid-state

photodetectors (MRS) to read out the WLS fibers, and then the performance of quad coincidence schema for the neighboring fibers of the formed cells. To avoid MRS high dark noise rate, rather high threshold (more than 3 photoelectrons (PE) ) was used for each photodiode. By moving the radioactive source across the cells, with MRS sensors being in coincidence schema, the optical width of the cell was measured. The direct coincidences realized between both WLS fibers on each side of the cell were similar to [7].

### III. DESCRIPTIONS AND SCHEMATICS

#### A. *Three Implemented Cell Formation Geometries*

As bases for all three cell formation geometries by using grooves, 20cm x 10cm x 5mm extruded scintillator pieces [8] were used. Initial pieces were solid, i.e. they didn't contain any co-extruded features like holes, etc. In order to optically separate the cells from each other, the following types of grooves were milled through the strips with a computer-controlled machine (THERMWOOD) at Fermi National Accelerator Laboratories (FNAL) Lab8: “key” grooves on the one side (Fig. 1a), “key” grooves on both sides – in alternating fashion (Fig. 1b), and “key” grooves on the one side and separation grooves on the other (Fig. 1c). The schematics and dimensions of the “key”-shape groove and rectangular separation groove are given in Fig. 1d. Each cell formed between two neighboring “key” grooves is 1cm wide and 20cm long.

#### B. *MRS Photodiode Description and Operational Principle*

The MRS photodiode is a multi-pixel solid-state device with every pixel operating in the limited Geiger multiplication mode. A resistive layer on the sensor's surface accomplishes avalanche quenching. The devices used were of round shape and had ~ 1000 pixels per 1.1mm diameter photosensitive area, with the quantum efficiency (QE) of the device reaching ~25% at 500nm [9]. In addition, MRS photodiodes are non-sensitive to the magnetic field [6]. Because the MRS gain is not high, we need to use an amplifier first and than a discriminator with 30 mV threshold.

## MRS-Scintillator Module Description

After tests described in experimental section, a “key” grooves on the one side and separation grooves on the other scintillator piece was selected as optimal in terms of cell separation for further tests with MRS photodiodes. The Kuraray [10] Y-11, 1.2mm diameter, WLS fibers were inserted into all ten “key” grooves without gluing, the scintillator was wrapped in Tyvek. Four MRS sensors were placed one on each side of two fibers marked 5 and 6 in the middle of the module and the amplifier was used (Fig. 2a). The MRS power circuit schematic is drawn in Fig. 2b.

## IV. EXPERIMENTAL SECTION

### A. *Choosing Cell Formation Geometry*

In order to choose the better cell formation geometry out of a solid scintillator piece, the following test was conducted for all three possibilities. For these tests on all three scintillator pieces, the groove being tested was connected via 1.15m long, 1.2mm diameter, Y-11, WLS Kuraray [10] fiber to the Hamamatsu [11] R580 photomultiplier tube (PMT). The PMT was connected to the Keithley [12] 6485 picoammeter that was read out by the computer. The  $^{90}\text{Sr}$  radioactive source was placed in the center position between grooves 5 and 6. After each measurement, the connected to PMT read-out fiber would be inserted into the next groove, with source being stationary. For the last test using “key” grooves on the one side and separation grooves on the other scintillator piece only, 20cm long WLS fibers were inserted into nine “key” grooves, with the groove under the tested connected to PMT via the same fiber. When the read-out fiber was moved from groove to groove, the short fiber would be removed from each next groove and inserted into previous, so there were no empty grooves left. The schematic for these tests is shown in Fig. 3a. The results of these tests are shown in Table I and are graphically represented in Fig. 3b.

Tests show that the “key” grooves on the one side and separation grooves on the other side provide better optical separation between the cells then for “key” grooves alone. The insertion of the fibers into empty grooves greatly improves the separation (by factor of  $\sim 2-3$ ) but also reduces the overall output ( $\sim 25\%$ ). To better understand this behavior, a scintillator piece of 10cm x 10cm x 5 mm with two equidistant from the center (at 2.5cm) co-extruded holes [8] was used with the setup in Fig. 3a. Three tests were carried out: one with two 1.15m fibers being inserted

into both holes and connected to PMT, one fiber inserted into one of the holes and connected to PMT with other hole empty, and both fibers inserted but only one connected to PMT. The  $^{90}\text{Sr}$  radioactive source was placed in the center of the scintillator and was stationary during entire test. The normalized average responses were 1.00, 0.60 and 0.51, with an error of 0.01. This illustrates the partial light loss when a WLS fiber presents in the neighboring hole or groove.

Since the “key” grooves on the one side and separation grooves on the other scintillator strip exhibited the best optical separation between the cells between the three samples, it was chosen for the test with MRS photodiodes.

### *B. MRS-Scintillator Cell Performance in Module*

The schematic for the module performance test is drawn in Fig. 4a. The double coincidences were organized between pairs of MRS photodiodes on each WLS fiber. In addition, double coincidence was organized between neighboring fibers, that for simplicity what be designated as quad coincidences. A visual scaler with three inputs was used to determine an average rate from each coincidence units over 60 seconds, with results converted into frequency.

Throughout measurements, a noise rate (i.e. without radioactive source but with base voltage on) was about 0.15 Hz for fiber coincidences and was  $\sim 0.15\text{Hz}$  and  $\sim 0.02\text{Hz}$  for coincidence between the fibers, small compared with value itself deviations for each measurement. Fig. 4b displays the results of the measurement. A radioactive source was moved by 2mm steps from position 120mm (what was closer to fiber 1) to position 84mm, with 100mm being equidistant between fibers 5 and 6. Data for fiber 5, fiber 6 and their coincidence are shown. Highest rate for double coincidences were when the source is directly above the corresponding fiber, and highest rate for quad coincidences is when the source is between fibers 5 and 6, as expected. Vertical Dashed lines in Fig.4b indicate positions of the fibers. Thus, only the quad coincidences define the cell elements in usable fashion.

The coincidences curve shape, between fibers 5 and 6, shows a well define width of the central cell even with non-collimated radioactive source. The effective width of cell may be slightly sensitive to the discrimination thresholds, which we are going to verify with beam particles.

## V. CONCLUSIONS

The idea of using extruded scintillating strip with co-extruded holes and separation grooves in 10 mm steps to create narrow cells in modular design was tested with extruded scintillating strip and machining grooves. The results indicate that performance of the module and electronically formed cells can be used in calorimetry and muon registration system with an area resolution about  $1 \text{ cm}^2$  using two modules with narrow cells oriented perpendicular to each other or defined by energy flow algorithms. The readout via short WLS fibers was performed without gluing and without clear fibers.

Overall, the results agree with the expectations and are essential to using in the calorimeter for the future international  $e^+e^-$  linear collider that is fully immersed in a strong magnetic field, or any other detector parts like tail-catcher or muon tracker that affects energy flow algorithms. ILC detector will require a large amount of scintillator at a reasonable price. Development of a low cost extruded scintillator strips can be done with co-extruded holes inside and co-extruded separation grooves outside, which are covered with co-extruded reflector. All together may simplify and speed up the assembly, metrology, and reduce the cost.

## VI. REFERENCES

- [1] V. Ammosov, "Status and plans of DHCAL RPC R&D in IHEP", [http://polywww.in2p3.fr/flc/general-meeting/desy-jan04/DHCAL/CALICE\\_IHEP\\_Jan\\_2004.ppt](http://polywww.in2p3.fr/flc/general-meeting/desy-jan04/DHCAL/CALICE_IHEP_Jan_2004.ppt).
- [2] A. White, "Digital Hadron Calorimetry Using Gas Electron Multiplier Technology." [http://www.hep.anl.gov/repond/lcws05\\_White.ppt](http://www.hep.anl.gov/repond/lcws05_White.ppt)
- [3] A. Dyshkant, D. Beznosko, G. Blazey, D. Chakraborty, K. Francis, D. Kubik et al., "Towards a Scintillator-Based Digital Hadron Calorimeter for the Linear Collider Detector", IEEE vol. 51, no. 4, pp.1590-1595, Aug. 2004.  
A. Dyshkant, D. Beznosko, G. Blazey, D. Chakraborty, K. Frances, D. Kubik et al, "Small Scintillating Cells as the Active Elements in a Digital Hadron Calorimeter for the e+e- Linear Collider Detector", FERMILAB-PUB-04/015, Feb 9, 2004
- [4] T. Takeshita, "GLD-Calorimeter", Snowmass 2005, <http://nicadd.niu.edu/cdagenda/fullAgenda.php?ida=a0561#s1>
- [5] D. Beznosko, G. Blazey, D. Chakraborty, A. Dyshkant, K. Francis, D. Kubik et al., "Investigation of a Solid State Photodetector", NIM A, Volume 545, Issue 3, 21 June 2005, Pages 727-737.
- [6] D. Beznosko, G. Blazey, A. Dyshkant, V. Rykalin, V. Zutshi, "Effects of the Strong Magnetic Field on LED, Extruded Scintillator and MRS Photodiode", accepted to NIM A (NIMA-D-05-00049), Jul 11, 2005
- [7] A. Akindinov, G. Bondarenko, V. Golovin, E. Grigoriev, Yu. Grishik, D. Mal'kevich et al., "Scintillating counted with MRS APD light readout", NIM A, 539 (2005) 172-176
- [8] D. Beznosko, A. Bross, A. Dyshkant, A. Pla-Dalmau V. Rykalin, "FNAL-NICADD Extruded Scintillator", FERMILAB-CONF-04-216-E, September 15, 04
- [9] M. Golovin, A. V. Akindinov, E. A. Grigorev, A. N. Martemyanov, P.A. Polozov, "New Results on MRS APDS", Nucl. Instrum. Meth. A387 231-234, 1997
- [10] Kuraray America Inc., 200 Park Ave, NY 10166,USA; 3-1-6, NIHONBASHI, CHUO-KU, TOKYO 103-8254, JAPAN.
- [11] Hamamatsu Corporation, 360 Foothill Road, PO Box 6910, Bridgewater, NJ 08807-0919, USA; 314-5,Shimokanzo, Toyooka-village, Iwata-gun, Shizuoka-ken, 438-0193 Japan
- [12] Keithley Instruments, Inc., 28775 Aurora Road, Cleveland, OH 44139, USA.

TABLE I  
FIBER RESPONSE FOR DIFFERENT CELL FORMATION GEOMETRIES\*

RESPONSE GROOVE #	FOR "KEY" GROOVES ON THE ONE SIDE (nA)	FOR "KEY" GROOVES ON BOTH SIDES – IN ALTERNATING FASHION (nA)	FOR "KEY" GROOVES ON THE ONE SIDE AND SEPARATION GROOVES ON THE OTHER (nA)	FOR "KEY" GROOVES ON THE ONE SIDE AND SEPARATION GROOVES ON THE OTHER WITH WLS FIBERS INSERTED (nA)
1	527.3	522.8	387.2	102.6
2	611.1	607.6	495.5	149.4
3	735.9	722.6	656	251.3
4	924.9	906	906.8	464.4
5	1175.2	1193.9	1238.4	853
6	1211.3	1230.2	1261.4	894.1
7	908.1	897.2	908.5	472.3
8	725.3	718.6	673.9	268
9	605.3	577	513.3	160.2
10	528.1	492.8	401.6	109.7

\* In all cases the dark current was less than 0.5 nA.

## Figure Captions:

Fig. 1a. Scintillator with “key” grooves on the one side.

Fig. 1b. Scintillator with “key” grooves on both sides – in alternating fashion.

Fig. 1c. Scintillator with “key” grooves on the one side (as in Fig. 1a) and separation grooves on the other.

Fig. 1d. “Key” groove (left) and separation groove (right). All dimensions in inches.

Fig. 2a. MRS-scintillator module setup.

Fig. 2b. MRS power circuit schematics. One channel is shown with common input power RC filter

Fig. 3a. Schematic of MRS-scintillator module readout by PMT. Radioactive source position is indicated by x.

Fig. 3b. Fiber response for different cell formation geometries.

Fig. 4a. MRS-scintillator module performance test schematic. Radioactive source was moved along the dotted line.

X marks the center of the strip.

Fig. 4b. Fiber 5, fiber 6 and coincidence between 5 and 6 rates with varying radioactive source position. Dashed lines across the X-axes represent exact position of the fibers with corresponding numbers indicated.



Fig. 1a.



Fig. 1b.

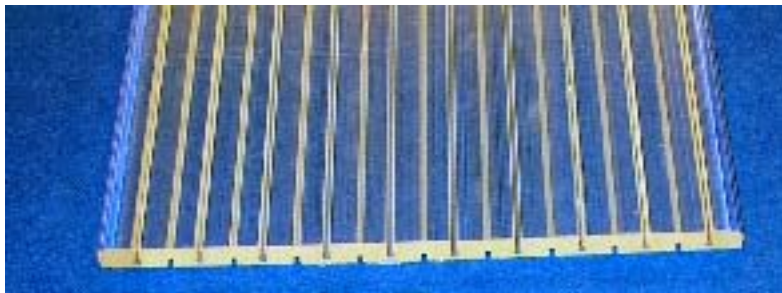


Fig. 1c.



Fig. 1d.

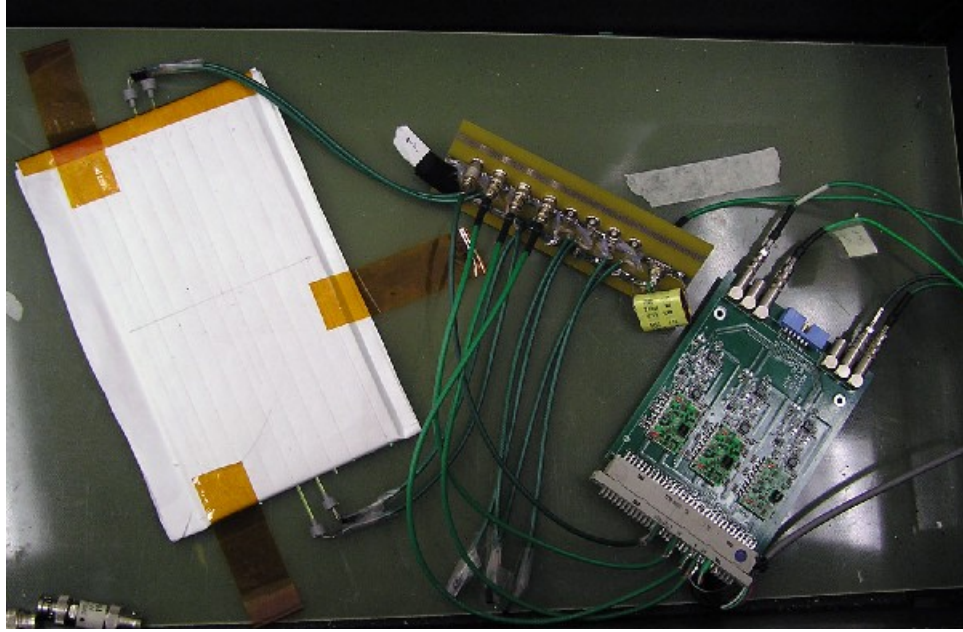


Fig. 2a.

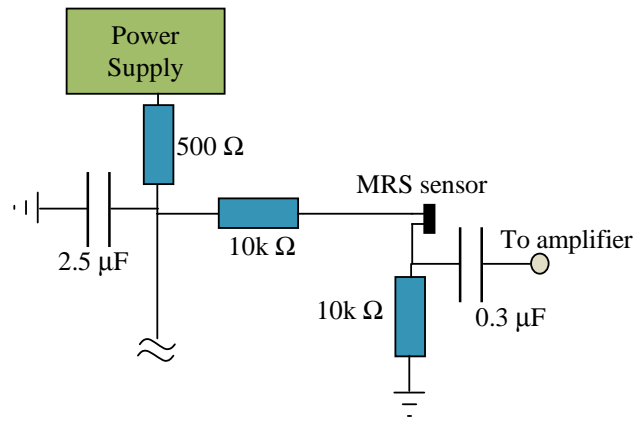


Fig. 2b.

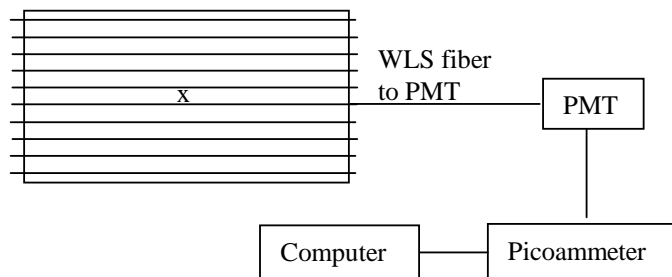


Fig. 3a.

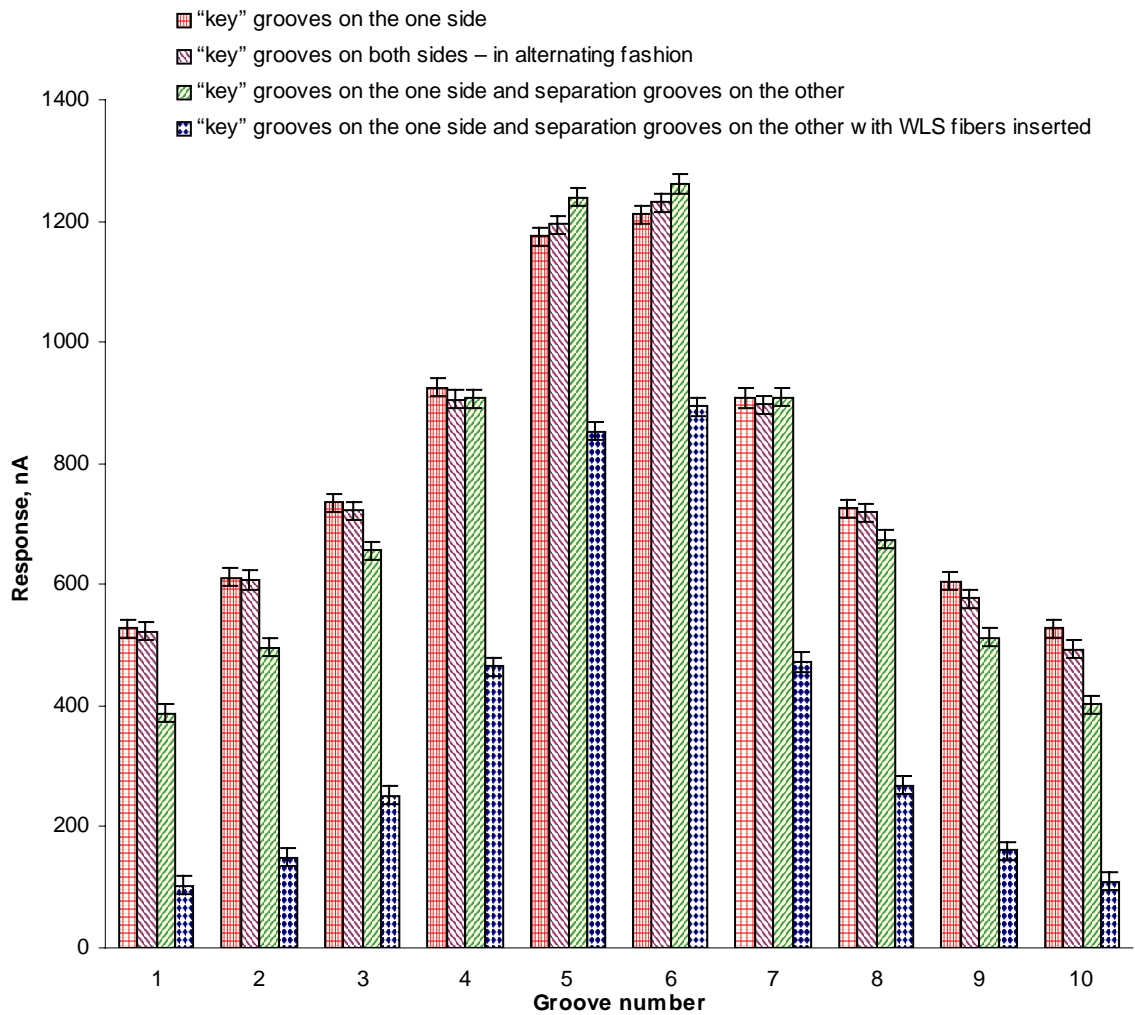


Fig. 3b.

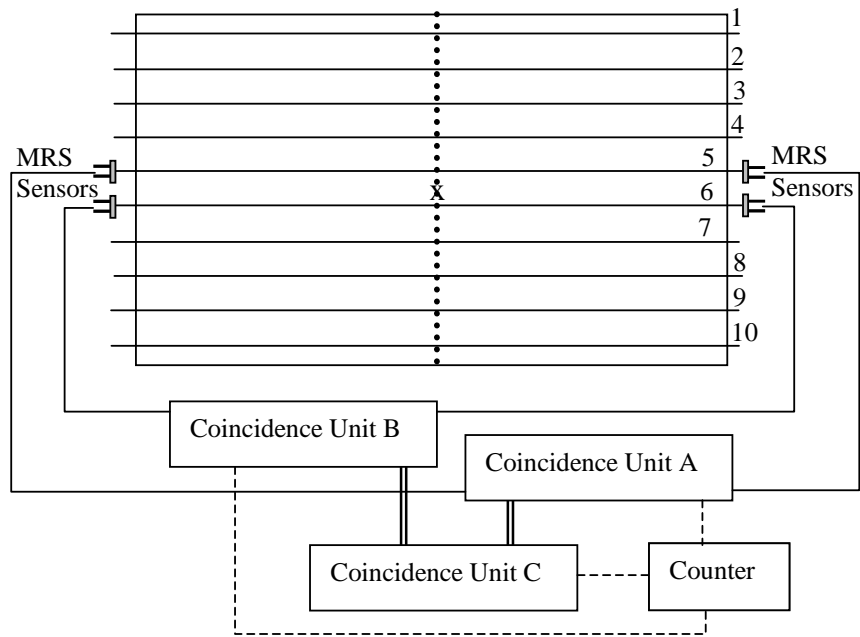


Fig. 4a.

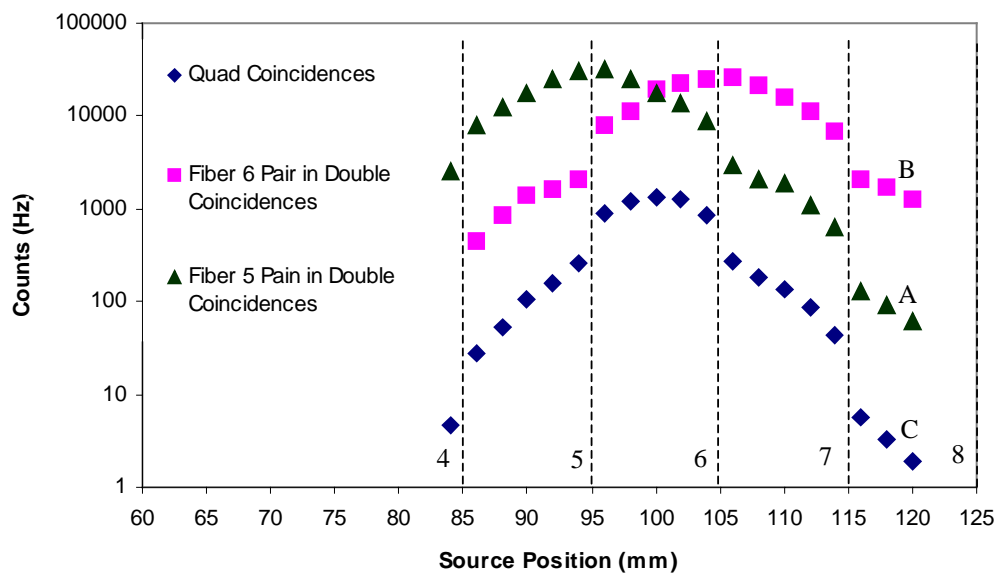


Fig. 4b